Pergamon

0956-7151(95)00015-1

Acta metall. mater. Vol. 43, No. 8, pp. 3075–3083, 1995
Elsevier Science Ltd
Copyright © 1995. Acta Metallurgica Inc.
Printed in Great Britain. All rights reserved
0956-7151/95 $9.50 + 0.00

THE INFLUENCE OF AN ORDERING TRANSITION ON THE INTERDIFFUSION IN Fe–Si ALLOYS

E. RABKIN[1], B. STRAUMAL[1,2], V. SEMENOV[2], W. GUST[1] and B. PREDEL[1]

[1]Max-Planck-Institut für Metallforschung and Institut für Metallkunde, Seestr. 75, D-70174 Stuttgart, Germany and [2]Institut of Solid State Physics, Russian Academy of Sciences, Chernogolovka, Moscow 142432, Russia

(Received 31 October 1994)

Abstract—The concentration dependencies of the interdiffusion coefficient $\tilde{D}$ have been measured with the aid of electron probe microanalysis at seven temperatures in the concentration interval 6–16 at.% Si near the concentration c_{ord} of the A2–B2 ordering transition. In ordered B2 phase the interdiffusion coefficient $\tilde{D}$ is about 2–3 times lower than in the disordered phase. Near the A2–B2 ordering transition $\tilde{D}$ depends strongly on the silicon concentration c. There is a maximum on every $\tilde{D}(c)$ dependence always shifted about 2–3 at.% Si to the left from c_{ord}. Such behaviour has been explained by the concentration dependence of the thermodynamic factor Φ. Dependencies $\Phi(c,T)$ have been calculated within the framework of the mean field theory (Bragg–Williams–Gorsky model), and the fluctuation contribution has been estimated using a scaling hypothesis. The calculated dependencies are in good agreement with the experimental data.

1. INTRODUCTION

The ordered alloys and intermetallic compounds have become very important as materials for producing parts working at high temperatures and in agressive environments [1–7]. The high strength of these materials is basically determined by the low diffusivity due to the atomic ordering. The existing diffusion data for these materials are not complete and show behaviour very different from the dilute alloys [8]. Dilute alloys can be adequately described using the self or tracer diffusion coefficients. For treating the diffusion-controlled properties of ordered alloys and intermetallics the interdiffusion coefficient $\tilde{D}$ must be used [7, 9, 10]. $\tilde{D}$ and in turn the diffusion-controlled properties depend strongly on the concentration [1], but the experimental data in this field are rather contradictory [8–14]. Another important open question is the behaviour of $\tilde{D}$ near the ordering phase transition. There is some experimental data showing very unusual deviations from Arrhenius law for $\tilde{D}$ near the ordering temperature [15–18].

Therefore it is very important to investigate experimentally the interdiffusion in the narrow concentration or temperature interval near the line of ordering phase transition on the phase diagram and to describe the behaviour of $\tilde{D}$ by the adequate thermodynamic model.

The goal of this work was to investigate the behaviour of the interdiffusion coefficient in the narrow concentration interval near the A2–B2 phase transition. For this purpose, we have measured the dependencies $\tilde{D}(c)$ with the high concentrational resolution and have discussed $\tilde{D}(c)$ pecularities using existing thermodynamic data. For the measurements and theoretical calculations we have chosen the A2–B2 ordering phase transition in the Fe–Si system because the phase diagram, Fe self-diffusion coefficients and thermodynamic data for this system are well established. The $c_{ord}(T)$ line for this transition lies practically vertical on the Fe–Si phase diagram. This enables us to investigate the $\tilde{D}$ behaviour very close to the ordering transition line because we can measure $\tilde{D}(c)$ dependencies instead of $\tilde{D}(T)$ ones. The $\tilde{D}(c)$ dependencies can be obtained with much higher resolution than the temperature dependencies. On the other hand, many technologically important ordered compounds like, for example, NiAl, CoAl, FeAl, also have the same B2 (CsCl) structure [1].

2. EXPERIMENTAL

This work is devoted to the investigation of bulk interdiffusion near the A2–B2 ordering phase transition in Fe–Si alloys. The Fe–5 at.% Si and Fe–25 at.% Si alloys were produced from Fe of 99.99% purity and from Si of 99.999% purity. After mixing in desired proportion the pressed powder samples underwent radio frequency levitation melting in vacuum. This technique uses no crucible and provides a homogeneous mixing of elements in the liquid state. The melt was cast into cylindrical copper moulds to form Fe–5 at.% Si and Fe–25 at.% Si rods. The Fe–5 at.% Si rods were used to grow cylindrical ⟨001⟩ single crystals about 10 mm in diameter by the electron beam zone floating technique [19]. The unit for electron beam zone melting described earlier [20] provides further refining of the material and uniform smooth distribution of the elements. The single crystals grown were oriented by Laue X-ray back-reflection. These

were cut to about 3 mm thick slices perpendicular to their axis. These slices were carefully polished on 4000 grit SiC paper and chemically etched in order to remove the surface damaged layer. After etching, the samples were annealed for 5 h at 1473 K in order to relieve any residual strain.

The Fe–25 at.% Si polycrystalline alloy was cut to pieces of thickness 0.5 mm. For making the diffusion couple a piece of Fe–25 at.% Si alloy was put in the electron beam installation on the top of a single crystalline Fe–5 at.% Si slice lying on the massive Mo substrate. To have a good coverage the single crystal had to be heated up to a temperature of about 1300 K. After that the electron beam was shortly (about 20 s) focused at the piece of Fe–25 at.% Si alloy heating it up to about 1600–1630 K (see Fig. 1). After the Fe–25 at.% Si alloy piece becomes liquid and forms a droplet on the top of the Fe–5 at.% Si alloy single crystal, the operator immediately shut the E-beam heating down, and the formed diffusion couple was cooled down very fast on the massive Mo substrate which remained cold during all the procedure. According to the Fe–Si phase diagram some Fe-rich alloy were diluted in the droplet of liquid Fe–25 at.% Si alloy. After cooling, the concentration of silicon in the applied layer was about 20 at.% Si (see Fig. 2). (Actually this concentration was a little bit different in different slices coated independently and lies between 18 and 20 at.% Si, see for example the left side of Fig. 4.) The distance between the positions of contact planes before and after heating was about 100 μm.

This applying procedure enables us to produce the perfect contact between both alloys. The diffusion couple (Fe–5 at.% Si)/(Fe–20 at.% Si) was formed after this procedure. Therefore, the c_{ord} concentration of the A2–B2 ordering transition lies in the concentration interval where the interdiffusion had to be studied in the narrow vicinity of c_{ord} (see Fig. 3 where the concentration and temperature intervals studied are shown). This enables us to 'stretch' the diffusion profiles and to enlarge the concentrational resolution of $\tilde{D}(c)$ dependencies near c_{ord} in order to obtain more information about $\tilde{D}$ pecularities near the ordering transition.

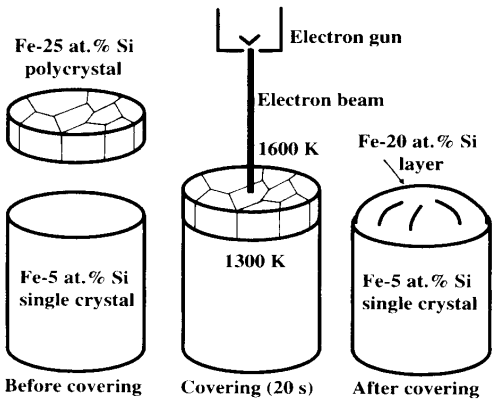

Fig. 1. The method of applying the Fe–20 at.% Si layer on the top of the Fe–5 at.% Si single crystal.

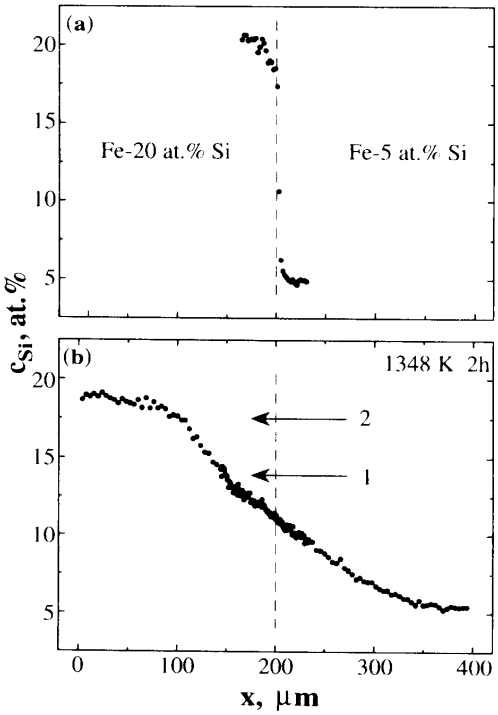

Fig. 2. Si concentration profiles in the diffusion couple before (a) and after (b) diffusional annealing.

It was important to control the thickness of the diffusional layer built between the halves of the diffusion couple during its preparation. The thickness of this layer should be negligible in comparison with the thickness of the diffusional layer after diffusion anneal because the solution for the couple with two infinite halves and constant concentrations should be

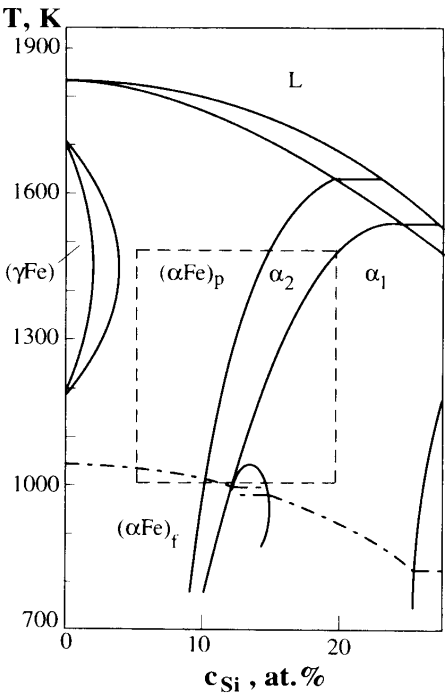

Fig. 3. Part of the Fe–Si phase diagram. The phase α-Fe has unordered A2 structure, the ordered α_2 phase has B2 (CsCl) structure and the ordered α_1 phase has DO_3 structure. The temperature and concentrational intervals studied are shown.

used. During the couple preparation ($t = 20$ s) the former contact plane moved about 100 μm due to the dissolution of Fe–5 at% Si alloy in the droplet of Fe–25 at.% Si alloy. The thickness x_0 of diffusional layer for diffusion from the plane with constant concentration c_0 moving with dissolution velosity v could be estimated using following equation [21]

$$c(x,t) = \frac{1}{2} c_0 \left[\operatorname{erfc} \frac{x + vt}{2\sqrt{\tilde{D}t}} + \exp\left(- \frac{vx}{\tilde{D}} \right) \operatorname{erfc} \frac{x - vt}{2\sqrt{\tilde{D}t}} \right]. \quad (1)$$

Here $\tilde{D}(c)$ is the interdiffusion coefficient for Fe–20 at.% Si alloy extrapolated to 1600 K using experimental data [22]. According to this equation $x_0 \approx 4$ μm. The measurements with the aid of electron probe microanalysis (EPMA) show (Fig. 2) that the thickness of the transition layer is really negligible in comparison with the thickness of the diffusional layer after anneal. The EPMA profiles show also that the Si concentration in the solidificated droplet is constant.

Our method of sample preparation permits us to investgate the interdiffusion in single crystals without the disturbing influence of GBs in the diffusion zone. Indeed, during the cooling down the liquid layer crystallizes on the Fe–5 at.% Si {001} single crystal like on the seed, and the monocrystal of alloy with 20 at.% Si grows. (Of course this single crystal of Fe–20 at.% Si alloy is not so perfect like the Fe–5 at.% Si substrate.)

Samples, approx. 2 × 3 × 7 mm in size, with 2 × 7 mm faces parallel to {001} were then cut using the electro-spark machine from the slices with applied Fe–20 at.% Si layer and encapsulated in silica ampoules under vacuum ($< 4 \times 10^{-4}$ Pa). These diffusion couples were than annealed at four different temperatures between 1006 and 1283 K (see Fig. 3). Other samples were annealed at four temperatures between 1483 and 1283 K in the vacuum resistance furnace ($< 10^{-4}$ Pa). After annealing the samples were mounted in Wood's metal and ground and polished through 1 μm diamond paste. The concentration profiles $c(x)$ (Figs 2 and 5) in the diffusion layer perpendicular to the contact plane were than determined. The EPMA measurements were carried out by wave length dispersive analysis on a JEOL 6400 electron probe microanalyser operated at 15 kV. The intensities of the FeK_α and SiK_α peaks were determined using 'PET' and LiF crystals, respectively. The Si and Fe concentrations were obtained utilizing a program which applied atomic number, absorbtion, fluorescence and background corrections.

The dependencies of the interdiffusion coefficient $\tilde{D}$ on the molar fraction of Si atoms should be then calculated using the concentration profiles $c(x)$. For the determination of concentration profiles the beam was stepped at 1 μm intervals. In the case when profiles were very long the beam was stepped at 1 μm intervals

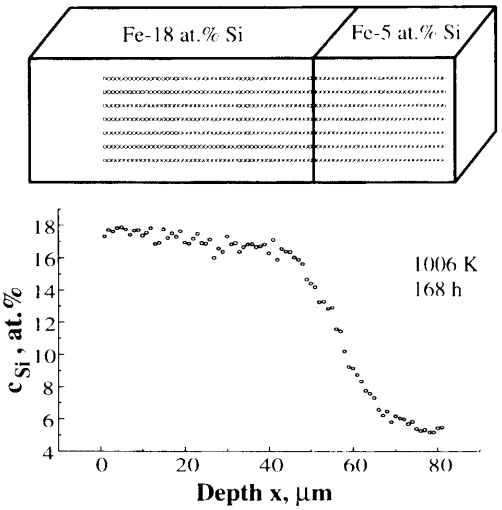

Fig. 4. Measurement of diffusion profiles. The position of the electron probe and the averaged concentration profile are shown.

only in the most interesting part of them, namely near c_{ord}, and at 2 or 3 μm intervals on the tails of profiles in order to conserve the measuring time for profile as not longer than 10–16 h. In order to improve the accuracy of $\tilde{D}(c)$ determination several (4–7) concentration profiles $c(x)$ were measured perpendicular to the contact plane (Fig. 4). The distance between the profiles was 10 μm. For the group of neighbouring profiles the averaged profile was then determined.

The averaged profiles were processed in order to determine the concentration dependence of the interdiffusion coefficient $\tilde{D}(c)$. We have employed the Boltzmann–Matano analysis for the calculation of $\tilde{D}(c)$. The method can be applied only if the Vegard's rule for the molar volume of alloys is valid. It has been shown recently [23] that even in the case of relatively strong deviations from the Vegard's rule (about 2%) the difference between the Boltzmann–Matano analysis and exact Sauer–Freise [24] analysis is negligible. Thus in the present work the Boltzmann–Matano method has been used. In order to smooth the experimental data, the concentration tails of the diffusion profiles were fitted by the error function, and the rest of the profile was smoothed by the four-point Fourier filter. The interdiffusion coefficient $\tilde{D}$ for the given Si concentration c^* at the given distance x^* was calculated according to the formula

$$\tilde{D}(c^*) = \left(2t \frac{\partial c}{\partial x}\Big|_{x^*} \right)^{-1} \int_{c_0}^{c^*} (x_M - x)\mathrm{d}c \quad (2)$$

where t is the time of the diffusional anneal, x is the distance and x_M denotes the position of the Matano place which is defined by

$$\int_{c_0}^{c_1} (x_M - x)\mathrm{d}c = 0 \quad (3)$$

where c_0 is the molar fraction of Si atoms in the Si-poor part of diffusion couple and c_1 the Si concentration in the Si-rich part.

3. RESULTS

The averaged concentration profiles $c(x)$ (Fig. 5) are shown for six temperatures investigated. The $c(x)$ profile for anneal at 1348 K, 2 h is shown in Fig. 2. All profiles have pronunciated deviations from the error function form typical for $\tilde{D}(c) = \text{const}$. For example, arrow 1 in Fig. 2 shows the strong change of $\tilde{D}$ at c of about 13 at.% Si. Between arrows 1 and 2 ($c > 13$ at.% Si) the interdiffusion coefficient $\tilde{D}$ is 2–3 times lower than at $c = (6\text{–}12$ at.% Si).

The concentration dependencies of the interdiffusion coefficient $\tilde{D}(c)$ determined using the procedure described above are shown in Fig. 6. Thick solid arrows show the concentration of A2–B2 ordering. Dotted arrows show the concentration of B2–DO_3 ordering. Thin arrow show the concentration of ferromagnetic–paramagnetic transition. The following features can be seen in these dependencies:

- There is a maximum on every $\tilde{D}(c)$ dependence (shown by the broken line going through all the $\tilde{D}(c)$ dependencies).
- This maximum is always shifted about 2–3 at.% Si to the left from the A2–B2 ordering concentration.

The concentration dependencies of formally determined activation energy $\tilde{Q}(c)$ and pre-exponential factor $\tilde{D}_0(c)$ are shown in Fig. 7(a) and (b), respectively. $\tilde{D}$ values at the temperature 1006 K have not been taken into account because of the influence

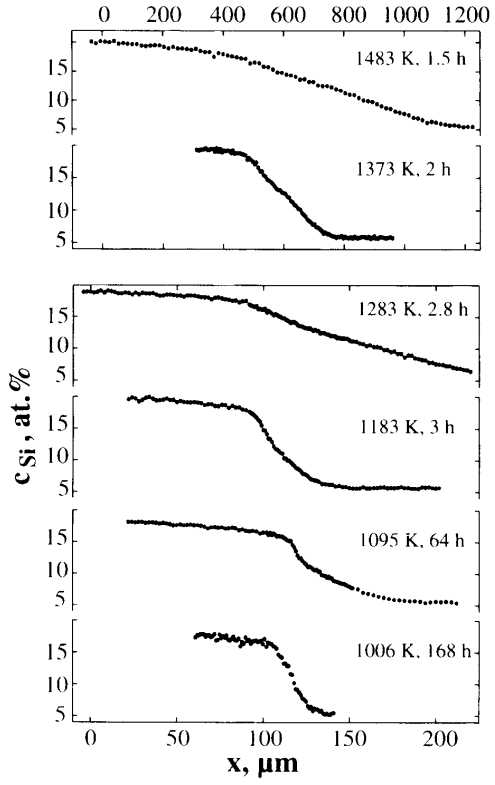

Fig. 5. Averaged concentration profiles.

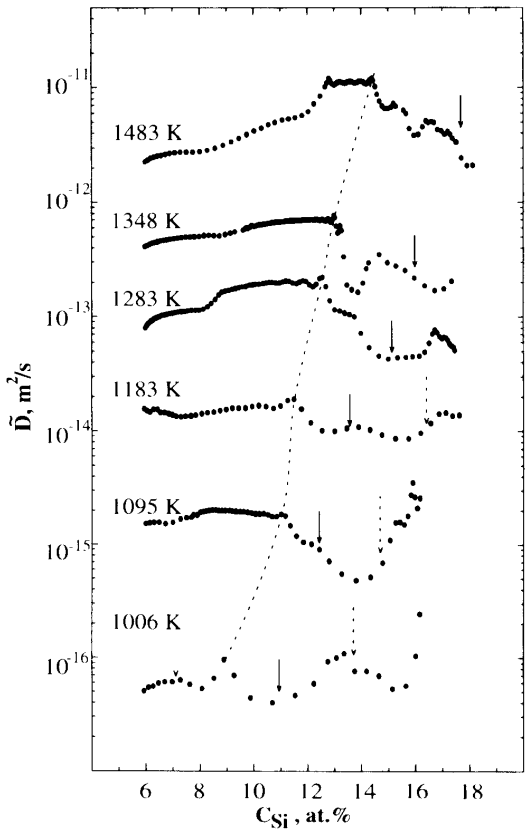

Fig. 6. Concentration dependencies of the interdiffusion coefficient. Thick arrows show the concentrations of A2–B2 ordering, dotted arows show the concentration of B2–DO_3 ordering, thin arrow show the concentration of the ferromagnetic–paramagnetic transition.

of the magnetic order on $\tilde{D}$ at that temperature. The solid circles show the quantities defined using only monotonous parts of the $\tilde{D}(c)$ dependencies (on the left side from the broken line on Fig. 6). The quadrats show the quantities determined using all the experimental data on both sides of the broken line. At low Si concentrations (in the disordered state, $c < 9$ at.% Si) $\tilde{Q}(c)$ and $\tilde{D}_0(c)$ nearly do not depend on c ($\tilde{Q} = 255 \pm 10$ kJ/mol and $\tilde{D}_0 = 10^{-3}$–10^{-2} m^2/s). Above $c \approx 9$ at.% Si the $\tilde{Q}(c)$ and $\tilde{D}_0(c)$ dependencies are nonmonotonous:

- At $c > 9$ at.% Si $\tilde{Q}$ and $\tilde{D}_0$ begin to grow.
- Above $c > 9$ at.% Si the quantities determined using all the experimental data grow faster than $\tilde{Q}$ and $\tilde{D}_0$ determined in the disordered region.
- $\tilde{Q}(c)$ and $\tilde{D}_0(c)$ dependencies have a maxima at $c \approx 13$ at.% Si [$\tilde{Q}(c) \approx 340$ kJ/mol and $\tilde{D}_0(c) \approx 10$ m^2/s]. We will see below, that the Arrhenius parameters for interdiffusion have a physical sense only in the interval of concentrations where the alloy is in the disordered or in the ordered state in the whole temperature interval studied.

4. DISCUSSION

According to Manning [25] the interdiffusion coefficient can be written as

$$\tilde{D} = (c\tilde{D}^*_{Fe} + (1 - c)\tilde{D}^*_{Si})\Phi r \qquad (4)$$

where $\tilde{D}_{Fe}$* and $\tilde{D}_{Si}$* are tracer self-diffusion coefficients of the components in homogenous Fe–Si alloy, Φ is the thermodynamic factor and r is the vacancy wind factor which is usually of the order of unity. It is known that tracer self-diffusion coefficients are changing in the ordered state [8]. In the case of magnetic ordering in α-Fe and its alloys the effect was thoroughly investigated [26, 27, 28]. Generally, tracer diffusion coefficients in the ordered ferromagnetic state are lower than it follows from the extrapolation of the Arrhenius line from the disordered paramagnetic region, and the activation energy for the diffusion far below the transition point is higher than in the disordered state. The same features of the self-diffusion coefficient temperature behaviour have also been observed in β-brass [29]. The physical reason for the increase in activation energy is the additional energy necessary for the breaking of atomic bonds in the ordered alloy at the formation and migration of a vacancy. Above the order–disorder transition temperature, the influence of the short-range order can be significant. Due to such influence, the temperature dependence of the tracer diffusion coefficient is smooth and downward deviations from the Arrhenius dependence begin above the transition temperature [27]. It is generally believed that qualitatively the principal features of the interdiffusion coefficient behaviour at the order–disorder transition are the same as for the tracer diffusion coefficients. However, present results show (see Fig. 6) that the interdiffusion coefficient changes abruptly rather than smoothly at the transition from disordered to ordered state, and such change occurs at a Si concentration when according to the equilibrium phase diagram the disordered phase is stable.

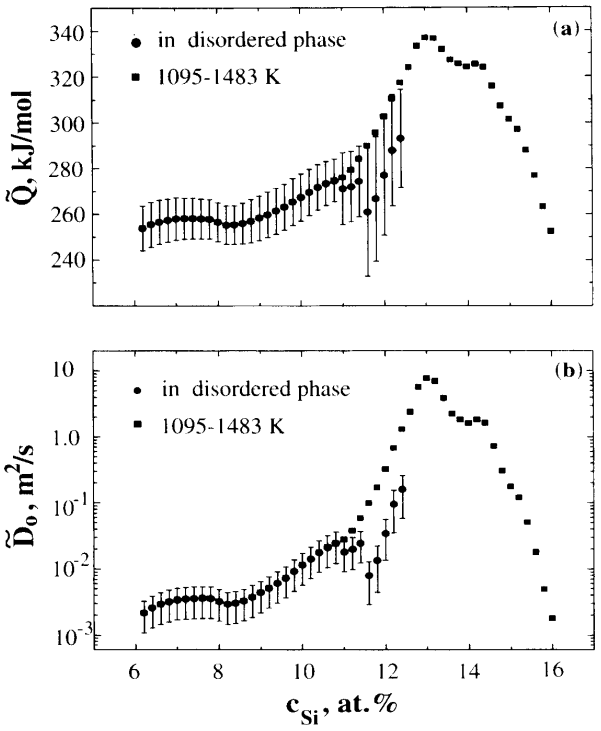

Fig. 7. Concentration dependencies of activation energy (a) and pre-exponential factor (b) of interdiffusion.

We will demonstrate below that the thermodynamic factor Φ is responsible for such behaviour of the interdiffusion coefficient. The thermodynamic factor expresses the tendency of an alloy to mixing or unmixing and can be written as [21]

$$\Phi = \frac{c(1-c)}{RT}\left(\frac{\partial^2 G}{\partial c^2}\right) \tag{5}$$

where G is the Gibbs energy of the alloy, R is the gas constant and T is the absolute temperature. It follows from equation (5) that Φ is proportional to the second derivative of the Gibbs energy of an alloy over concentration. Therefore, it should be connected with the other thermodynamic quantities, like specific heat, which exhibits so-called λ-singularity in the vicinity of the transition point. We will calculate below the thermodynamic factor in the mean-field approximation and show how the calculated behaviour changes in the narrow vicinity of the transition point.

4.1. Calculation of the thermodynamic factor in the mean field approximation

For the calculation of Φ the Gibbs energy of an alloy should be calculated firstly. According to Inden and Pitsch [30], the enthalpy of the FeSi alloy can be written as

$$H = \frac{1}{2}R\{(8W - 6w)x^2 + 3wy^2\} + Rc(1-c)(4W + 3w) \tag{6}$$

where W is connected with the nearest neighbour bond energies V

$$W = -2V_{FeSi} + V_{FeFe} + V_{SiSi} \tag{7}$$

and w with the next nearest neighbour bond energies v

$$w = -2v_{FeSi} + v_{FeFe} + v_{SiSi}. \tag{8}$$

Here, we have introduced two long-range order parameters x and y which are connected with the occupation probabilities of different sites in the lattice. If $x = 0$ and $y = 0$ we have the disordered body-centred cubic solid solution (A2 phase), situation $x > 0$, $y = 0$ corresponds to the ordered B2-phase, and the situation $x > 0$, $y > 0$ corresponds to the ordered $D0_3$ phase. At the calculation of the entropy S of the alloy the random distribution of atoms in every sublattice of the ordered structure is assumed

$$\begin{aligned} S = -\frac{R}{4}[&2(1-c+x)\ln(1-c+x) \\ &+ 2(c-x)\ln(c-x) \\ &+ (1-c-x+y)\ln(1-c-x+y) \\ &+ (c+x-y)\ln(c+x-y) \\ &+ (1-c-x-y)\ln(1-c-x-y) \\ &+ (c+x+y)\ln(c+x+y)]. \end{aligned} \tag{9}$$

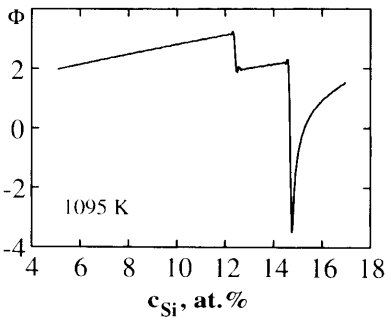

Fig. 8. Concentration dependence of the thermodynamic factor at 1095 K.

Combining equations (3) and (6) one can calculate the Gibbs energy of the alloy as a function of the concentration c, temperature T and order parameters x and y

$$G = H - TS. \tag{10}$$

The free energy should be minimized with respect to x and y at the given T and c in order to determine the actual values of the order parameters. We have used the following values of parameters [30]: $W/R = -2010$ K and $w/R = -1000$ K. After calculation of G, the thermodynamic factor can be calculated according to equation (5). A similar procedure has been used by Paidar at the calculation of the spinodal line for Fe–Si alloys [31]. The $\Phi(c)$ dependence for the temperature 1095 K is shown in Fig. 8. The dependence exhibits a step at the concentration corresponding to the A2–B2 phase transition and a deep sharp minimum at the concentration of the B2–$D0_3$ phase transition. The latter is connected with the fact that the mean field theory predicts the B2–$D0_3$ phase transition to be of the first order. However, experimental observations indicate that above 980 K it is of the second order, which can be connected with the high values of the energy of interfaces between B2 and $D0_3$ phases, which was not taken into account in equation (10) [32]. Thus, the most important conclusion for us is that the thermodynamic factor decreases abruptly by a factor of two at the transition from disordered to ordered phase.

4.2. *Beyond the mean field approximation*

The mean field approximation fails in the narrow vicinity of the phase transition point, where fluctuations of the order parameter are important [33]. In that so-called fluctuation region second derivatives of the free energy have characteristic λ-singularities. Φ should have the singularity in the fluctuation region, too, as was first pointed out with respect to the surface diffusion [34]. Consider that question in more details. According to the scaling theory [33], the fluctuation part of the Gibbs energy G_f depends on temperature by the power law

$$G_f = -A(c)|T - T_c|^{\nu d} \tag{11}$$

where $A(c)$ is a non-singular function of concentration, ν is the critical index for the correlation radius and d is the dimensionality of the system (2 or 3). Using the standard thermodynamic relation for the specific heat measured at constant pressure

$$C_p = -T\left(\frac{\partial^2 G}{\partial T^2}\right)_p \tag{12}$$

and combining equations (11) and (12), one can get for the anomalous part of the specific heat C_p^f

$$C_p^f = TA(c)|T - T_c|^{\nu d - 2} \tag{13}$$

where $\nu d - 2 = -\alpha$ is the critical index for the specific heat. Usually, the value of index α is close to zero, but the corresponding λ-singularities can be clearly observed. If the system is not too close to the critical point of the transition, one can write

$$|T - T_c| = |c - c_c|\left(\frac{\partial T}{\partial c}\right)_e \tag{14}$$

where the index e at the derivative denotes the derivative along the equilibrium phase transition line, and c_c is the concentration of Si at which the phase transition occurs. Combining equations (5), (11) and (14) one can get for the most singular fluctuation part Φ_f of the thermodynamic factor

$$\Phi_f = -\frac{c(1-c)}{RT} A(c)\left(\frac{\partial T}{\partial c}\right)_e^2 |T - T_c|^{\nu d - 2}. \tag{15}$$

Comparison of equations (13) and (15) shows that the thermodynamic factor has the same singularity as the specific heat, but with the opposite sign (v-type singularity). Specific heats of the Fe–Si alloys have been measured over a wide range of concentrations and temperatures [35]. The temperature dependence of the C_p at the fixed Si concentration exhibits definitely two λ-points at the A2–B2 and B2–$D0_3$ phase transition temperatures. Both the amplitude and the width of the anomalies increase with the temperature increase. It is clear from the above that the same features could be expected on the temperature and concentration dependencies of the thermodynamic factor.

4.3. *Comparison with the experiment*

The compiled concentration behaviour of the thermodynamic factor for the temperature 1373 K is shown on Fig. 9(b). The thin line exhibits Φ values calculated in the mean field approximation. The thick solid line shows the fluctuation contribution to the thermodynamic factor, and it can be represented as a converted λ-singularity of the specific heat. The resulting curve exhibits the maximum, which is shifted from the order–disorder transition concentration to the side of lower Si content and a minimum at the transition point. On Fig. 9(a) the concentration dependence of the interdiffusion coefficient for the

same temperature is shown, exhibiting the minimum at the phase transition point and a maximum shifted to the left from the transition point. A good qualitative agreement between two concentration dependencies can be seen. Thus, the concentration behaviour of the thermodynamic factor explains the two principal features of the concentration behaviour of the interdiffusion coefficient: the maximum at these dependencies shifted to the left form the order–disorder transition concentration followed by the rapid decrease of the interdiffusion coefficient at higher concentrations. It can also be seen from Fig. 6 that the shift of maxima on $\tilde{D}(c)$ dependencies increase with the temperature increase. It is in accordance with the widthening of the λ-anomaly of the specific heat at the temperature increase [35].

The same principal features of the concentration behaviour of interdiffusion coefficients have been observed earlier at the study of Fe–Al interdiffusion in the temperature interval 1173–1373 K and concentration interval 2–50 at.% Al [36]. However, the maxima on the $\tilde{D}(c)$ dependencies were interpreted as the manifestation of the A2–B2 order–disorder phase transformation, in spite of the fact that these maxima were also shifted to the side of lower Al concentration. Another possible reason for such a shift is the non-equilibrium character of the diffusion zone. It is known that in the diffusion zone the phase boundaries can differ from those in the equilibrium phase diagram, and some phases, especially with the narrow homogeneity region can not appear at all [21]. The non-equilibrium defects in the diffusion zone such as vacancies and dislocations can shift the phase boundary between ordered and disordered phase. It was shown recently [37], that the long-range order

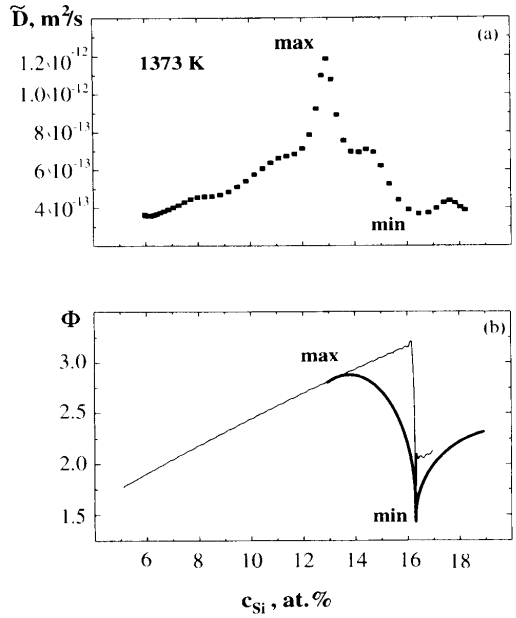

Fig. 9. The concentration dependence of the interdiffusion coefficient at 1373 K (a) and the compiled concentration behaviour of the thermodynamic factor at the same temperature (b).

parameter in the ordered Ni_3Al alloy can be reduced by a factor of 5 at the cold rolling. The decrease of the order parameter was attributed by the high density of structural defects in the deformed material. Thus, the non-equilibrium defects can only decrease the region of stability of the ordered phase. In our case it would lead to the shift of the maxima on the $\tilde{D}(c)$ dependencies in the direction of the high Si concentrations, which is not the fact.

It is clear from the above that the activation energy for interdiffusion has no physical sense at the Si concentrations above 11–12 at.%. Unphysically high values of the activation energy (up to 330 kJ/mol) and the pre-exponential factor (up to 10 m^2/s), see Fig. 7, can be explained by the strong concentration and temperature dependence of Φ. Values of the activation energy and pre-exponential factor in the disordered region at low Si concentrations (255 ± 10 kJ/mol and 10^{-3}–10^{-2} m^2/s) are in good agreement with the data of [38], where the interdiffusion coefficient in Fe–Si alloy was measured in the temperature interval 1073–1673 K at Si concentrations below 8 at.%: 249 kJ/mol and 1.7–3.5 10^{-3} m^2/s. Such values are characteristic for self-diffusion in Fe and its dilute alloys. Mirani and Maaskant [39] reported somewhat lower values of the activation energy and pre-exponential factor (210–215 kJ/mol and 1.6–1.8 10^{-4} m^2/s) for the temperature interval 1173–1373 K and for the Si concentrations from 8.35 to 10.41 at.%. That discrepancy can be connected with the non-equilibrium processes in the diffusion zone: the role of such processes increases as the difference in concentration between two samples constituting the diffusion zone increases. The arbitrary assumption $\tilde{D}_{Fe}^* = 0.2\tilde{D}_{Si}^*$ made in [39] at calculations should also be thoroughly investigated.

In our previous work [40] the $\tilde{D}(c)$ dependencies for Cu–Au alloys in the vicinity of A1–$L1_2$ ordering transition (Cu_3Au composition) has been determined. It was shown that up to 20 K below the critical temperature of phase transition (663 K) there are maxima on these dependencies approximately at the Cu_3Au composition. We have attributed these maxima also to the corresponding maxima on the concentration dependencies of the thermodynamic factor, which we have calculated in the frameworks of the tetrahedron approximation of the cluster variation method. The existence of such maxima has been proved also by the pair approximation of the cluster variation method [41] and Monte-Carlo simulations [42]. In the case of Fe–Si alloys, contrary to the Cu–Au alloys, the thermodynamic factor only decreases at the transition to the ordered state. We can illustrate the reason for that opposite behaviour by the simple free energy construction (Fig. 10). In the ordered state, an additional negative contribution to the free energy of the alloy appears, which is connected with the long-range order (shaded area in Fig. 10). In the Cu–Au alloy the concentration interval of the ordered phase stability is narrow, disordered phase being

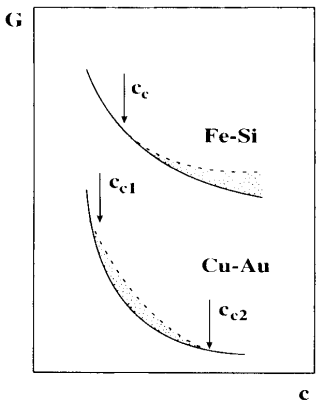

Fig. 10. The negative contribution to the free energy in the ordered state (shaded area) for the A2–B2 ordering in the Fe–Si system and for A1–$L1_2$ (Cu_3Au) ordering in the Cu–Au system.

stable both at low and high Au concentration. That leads to the increase of the second derivative (curvature) of the free energy vs concentration in the middle of the ordered region (Fig. 10). In the Fe–Si alloys the A2–B2 phase transition is followed by another ordering transition, B2–$D0_3$. The region of stability of the ordered phase is high, being bound at the side of high Si concentrations by the wide two-phase region. That leads to the decrease of the curvature of the free energy vs concentration dependence and corresponding step-like decrease of the thermodynamic factor. Thus, the difference in diffusion behaviour of the Fe–Si and Cu–Au alloys is attributed by the different types of phase diagrams.

5. CONCLUSIONS

From the results of this study following conclusions can be drawn.

1. The interdiffusion coefficient $\tilde{D}$ has been determined for Fe–Si single crystalline alloys in the concentration range 5–18 at. % Si and temperature interval 1006–1483 K.

2. The concentration dependencies of the interdiffusion coefficient show the following features:

- Up to some critical concentration the interdiffusion coefficient grows monotonically with the Si concentration increase.
- At Si concentrations higher than critical the interdiffusion coefficient falls rapidly; its value in the ordered region is 2–3 times lower than in the disordered one.
- The critical concentration is shifted from the A2–B2 phase transition concentration to the lower Si content.

3. The thermodynamic factor Φ has been calculated in the mean field approximation, and the fluctuation contribution to Φ has been estimated. The compiled $\Phi(c)$ behaviour is in a good agreement with the observed $\tilde{D}(c)$ dependencies.

4. It is shown that the Arrhenius parameters of the interdiffusion have no physical sense in the interval of concentrations where the order–disorder phase transition occurs. The thermodynamic factor contributes strongly to the temperature dependence of the interdiffusion coefficient in the vicinity of phase transition. The Arrhenius parameters for the interdiffusion in the disordered region (5–11 at.% Si) has been determined (255 ± 10 kJ/mol and 10^{-3}–10^{-2} m^2/s).

5. It is shown that the difference in the concentration behaviour of the interdiffusion coefficient in Fe–Si and Cu–Au alloys is attributed by the different width of the region of the ordered phase stability on corresponding phase diagrams.

Acknowledgements—This work was supported by the Volkswagen Foundation under contract I/69 000. E.R. wishes to thank the Alexander-von-Humboldt Foundation for support during this study. Professors L. Shvindlerman, V. Glebovsky and V. Paidar are greatly acknowledged for helpful discussions.

REFERENCES

1. M. H. Yoo, S. L. Sass, C. L. Fu, M. J. Mills, D. M. Dimiduk and E. P. George, *Acta metall. mater.* **41,** 987 (1993).
2. L. A. Johnson *et al.* (editors), *High-Temperature Ordered Intermetallic Alloys IV*, MRS Symp. Proc., Vol. 213. MRS (1991).
3. C. T. Liu *et al.* (editors), *Ordered Intermetallics-Physical Metallurgy and Mechanical Behavior*, NATO ASI Series E: Applied Sciences, Vol. 213. Kluwer Academic, Boston, Mass. (1992); M. Yamaguchi and Y. Umakoshi, *Prog. Mater. Sci.* **34,** 1 (1990).
4. L. E. Tanner and L. Wuttig. *Mater. Sci. Engng A* **127,** 137 (1990).
5. D. Caillard, J. Thibault and P. Veyssiére, *J. Physique* **1,** 829 (1991).
6. C. T. Liu, *Scripta metall. mater.* **25,** 1231 (1991).
7. D. B. Miracle, *Acta metall. mater.* **41,** 649 (1993).
8. H. Mehrer (editor), *Diffusion in Solid Metals and Alloys*, Landolt-Börnstein New Series, Vol. III/26. Springer, Berlin (1992).
9. R. D. Field, D. F. Lahrman and R. Darolia, *Acta metall. mater.* **39,** 2951 (1991).
10. A. Lasalmonie, *J. Mater. Sci.* **17,** 2419 (1989).
11. F. C. Nix and F. E. Jaumont, *Phys. Rev.* **83,** 1275 (1951).
12. G. F. Hancock and B. R. McDonell, *Physica status solidi* (a) **4,** 143 (1971).
13. S. Shankar and L. L. Seigle, *Metall. Trans. A* **9,** 1467 (1978).
14. W. Sprengel, M. Denkinger and H. Mehrer, *Intermetallics* **2,** 127 (1994).
15. I. Richter and M. Feller-Kniepmeier, *Physica status solidi* (a) **68,** 289 (1981).
16. O. I. Noskovich, E. I. Rabkin, V. N. Semenov, B. B. Straumal and L. S. Shvindlerman, *Acta metall. mater.* **39,** 3091 (1991).
17. E. I. Rabkin, L. S. Shvindlerman and B. B. Straumal, *J. less-common Metals* **158,** 23 (1990).
18. E. I. Rabkin, L. S. Shvindlerman and B. B. Straumal, *J. less-common Metals* **159,** 43 (1990).
19. V. G. Glebovsky, S. I. Moskvin and V. N. Semenov, *J. Cryst. Growth* **59,** 450 (1982).
20. V. G. Glebovsky, V. V. Lomeyko and V. N. Semenov, *J. less-common Metals* **117,** 385 (1986)
21. J. Philibert, *Atom Movements—Diffusion and Mass*

Transport in Solids, p. 9. Les Editions de Physique, Les Ulis (1991).
22. M. Onishi and H. Mitani, *Kinzoku Hyomen Gijutzu* **19,** 146 (1968).
23. W. Sprengel, M. Denkinger and H. Mehrer, *Intermetallics* **2,** 137 (1994).
24. F. Sauer and V. Freise, *Z. Elektrochem.* **66,** 353 (1962).
25. J. R. Manning, *Phys. Rev. B* **4,** 1111 (1971).
26. G. Hettich, H. Mehrer and K. Maier, *Scripta metall.* **11,** 795 (1977).
27. H. V. Mirani, R. Harthoorn, T. J. Zoorendonk, S. J. Helmenhorst and G. de Vries, *Physica status solidi* (a) **29,** 115 (1975).
28. J. Kucera, B. Kozak and H. Mehrer, *Physica status solidi* (a) **81,** 497 (1984).
29. A. B. Kuper, D. Lazarus, J. R. Manning and C. T. Tomizuka, *Phys. Rev.* **104,** 1936 (1956).
30. G. Inden and W. Pitsch, *Z. Metallk.* **62,** 627 (1971).
31. V. Paidar, *Czech. J. Phys. B* **27,** 50 (1977).
32. G. Schlatte and W. Pitsch, *Z. Metallk.* **67,** 462 (1976).
33. H. E. Stanley, *Introduction to Phase Transitions and Critical Phenomena*, p. 172. Clarendon Press, Oxford (1971).
34. L. A. Bol'shov and M. S. Vestchunov, *J. Exp. Teor. Fiz.* **95,** 2039 (1989).
35. H. H. Ettwig and W. Pepperhof, *Z. Metallk.* **63,** 453 (1972).
36. K. Nishida, T. Yamamoto and T. Nagata, *J. Japan Inst. Metals* **34,** 595 (1970).
37. J. Ball, R. Mitteau and G. Gottstein, in *Ordering and Disordering in Alloys* (edited by A. R. Yavari), p. 138. Elsevier, New York (1991).
38. A. Vignes, J. Philibert, M. Badia and J. Levasseur, *Trans. 2nd Nat. Conf. El. Microprobe Anal.*, Boston, 1967, Paper Nr. 20.
39. H. V. M. Mirani and P. Maaskant, *Physica status solidi* (a) **14,** 521 (1972).
40. B. Straumal, E. Rabkin, W. Gust and B. Predel, *Acta metall. mater.* **43,** 1817 (1995).
41. C. C. Wang and S. A. Akbar, in *Diffusion in Ordered Alloys* (edited by B. Fultz *et al.*), p. 3. TMS, Warrendale, Pa (1993).
42. L. Zhang, W. A. Oates and G. E. Murch, *Phil. Mag. A* **58,** 937 (1988).